



LUND UNIVERSITY
Faculty of Science

A comparison of modelled precipitation in Greenland

Author:
Rebecca VESTERBERG

Supervisors:
Elna HEIMDAL NILSSON
Ruth MOTTRAM

THESIS SUBMITTED FOR THE DEGREE OF BACHELOR OF SCIENCE

DEPARTMENT OF PHYSICS AT LUND UNIVERSITY

DANISH METEOROLOGICAL INSTITUTE

PROJECT DURATION: 2 MONTHS

DECEMBER 2017



Danmarks
Meteorologiske
Institut

Abstract

The Greenland ice sheet develops throughout the year with the changing weather conditions. Precipitation contributes by increasing the mass, whilst warmth induces melting, which makes the ice sheet diminish. The term Surface Mass Balance (SMB) is used for the isolated gain (accumulation) and melting (ablation) of the surface of the ice sheet and is therefore important for understanding future rates of sea level rise. This study compares the modelled precipitation from Regional Climate Model (RCM) HIRHAM5 and the Numerical Weather Prediction (NWP) model HIRLAM 7.3 to assess the challenges for RCMs and NWP models to accurately simulate accumulation rates on a local scale and the consequent impact on SMB uncertainty. It is concluded that HIRLAM 7.3 is an overall wetter model than HIRHAM5 for the studied region. One noticeable bias come from the different physiographic fields of orography, mountain like terrain, in the two models. It is also suggested that future studies should compare model output with observations to further assess model biases.

Acknowledgement

First and foremost, I would like to thank my supervisors Dr. Ruth Mottram at the Department of Climate and Arctic Research at the Danish Meteorological Institute (DMI) and Dr. Elna Heimdal Nilsson at the Department of Physics at Lund University. Ruth, who provided insight and expertise that greatly assisted the research and for inviting me to participate in many workshops and seminars. Elna, for her support and guidance during my diploma work and throughout all my years at Lund University. A big thank you to all the wonderful people at the office for making me feel welcome, and for sharing your pearls of wisdom with me during the course of this research. A special thanks to Fredrik Boberg, at the Department of Climate and Arctic Research at the DMI in Denmark for helping me with the programming!

This thesis was carried out at DMI using operational data products. Supervisory support was carried out by Dr. Ruth Mottram under the ERC Synergy project ice2ice (ERC grant no. 610055) from the European Union's Seventh Framework Programme (FP7/2007-2013) and the RETAIN project, funded by the Danish Council for Independent research (Grant no. 4002-00234). Additional data was produced at DMI by Dr. Kristian Pagh Nielsen, under the HIRLAM-C consortium.

This thesis is an individual extension of projects at DMI. This implies that papers on similar outcome and research could be found in future publications.

List of principal symbols and abbreviations

Abbreviations

AMAP:	A rctic M onitoring and A ssessment P rogramme
CDO:	C limate D ata O perator
DMI:	D anmarks M eteorologiske I nstitut (D anish M eteorological I nstitute)
ECMWF:	E uropean C entre for M edium- R ange W eather F orecasts
GHG:	G reen H ouse G as
GRIB:	G ridded B inary or G eneral R egularly-distributed I nformation in B inary form
HIRHAM:	H Igh R esolution H Amburg C limate M odel
HIRLAM:	H Igh R esolution L ocal A rea M odelling
IPCC:	I ntergovernmental P anel on C limate C hange
IR:	I nfra R ed radiation
NetCDF:	N etwork C ommon D ata F orm
NWP:	N umerical W eather P rediction
RCM:	R egional C limate M odel
SMB:	S urface M ass B alance
WMO:	W orld M eteorological O rganization

Symbols

$a:$	Radius of the Earth [m]
$c:$	Speed of light [m/s]
$C_p:$	Specific heat [$\text{J kg}^{-1} \text{K}^{-1}$]
$E:$	Energy [J]
$F_r:$	Frictional Force [N]
$g:$	Gravitational acceleration constant [9.82 m/s^2]
$h:$	Planck constant [$6.626110^{-34} \text{ Js}$]
$I:$	Intensity [W/m^2]
$p:$	Pressure [Pa]
$q:$	Specific humidity [-]
$Q:$	Heat [J]
$R:$	Specific gas constant [$287 \text{ Jkg}^{-1} \text{K}^{-1}$]
$T:$	Total temperature [K]
$u:$	East-west wind (x-direction) >0 towards the east [m/s]
$v:$	North-south wind (y-led) >0 towards the north [m/s]
$w:$	Vertical wind >0 upwards (z-led) [m/s]
$\Omega:$	Rotation rate of the Earth [rad/s]
$\Phi:$	Latitude [degrees]
$\rho:$	Density [kg/m^3]
$\sigma:$	Stefan Boltzmanns constant [$5.67 \times 10^{-8} \text{ WK}^{-4} \text{m}^{-2}$]
$\lambda:$	Wavelength [m]
$\lambda_m:$	The wavelength at which a blackbody radiates most strongly [m]

Contents

1	Introduction	1
2	Bakground	2
2.1	Climate change	2
2.2	Greenland ice sheet	4
2.3	Surface mass balance and dynamic mass loss	5
2.4	Climate and weather models	6
3	Method	8
3.1	HIRLAM 7.3 - Regional weather prediction model	8
3.2	HIRHAM5 - Regional climate model	8
3.3	Data analysis	9
4	Result and Discussion	10
4.1	Model output of precipitation	10
4.2	Extreme precipitation event October 2016	12
4.3	Topography	16
5	Conclusions and Outlook	19
6	Bibliography	20
7	Appendix	22

1 Introduction

The global climate is changing. The Earth is facing increasing average surface temperatures in both atmosphere and oceans, the amount of ice and snow is reduced, sea levels are rising, and concentrations of greenhouse gases (GHG) are increasing.

Because of the climate changes the Greenland ice sheet has been a focus of much research during the recent years. In this thesis the Greenland ice sheet mass change due to dynamical and surface processes is assessed. The concept of Surface Mass Balance (SMB) is calculated as the difference between accumulation and ablation. Accumulation is the positive mass term including precipitation, condensation and refreezing. Ablation is the negative mass term consisting of melt of the ice. The SMB determines the growth or decay of an ice sheet and is therefore important for understanding both ice dynamics and future rates of sea level rise. The Greenland ice sheet is known to be the second largest land ice mass on the planet, with around 2.85 million km³ of ice on an area of 1.71 million km², equivalent to 7.2 m sea level rise (IPCC, 2013). The Arctic has been warming more than twice as rapidly than the world as a whole for the past 50 years (AMAP, 2017) and at the same time increasing surface melt in Greenland has led to ever higher losses of mass from the ice sheet. This melt is due partly to higher temperatures and also changes in weather, such as precipitation variabilities, warm air masses and clearer skies during summer enhancing melt through albedo effect (Box et al., 2012; Tedesco et al. 2013; Hanna et al. 2013; Doyle et al. 2015). For each additional year of data, it becomes increasingly clear that the Arctic as we know it is being replaced by a warmer, wetter, and more variable environment. This transformation has profound implications for people, resources, and ecosystems worldwide. As the snow and ice in Arctic lessen, the ability to reflect heat back to space is reduced, accelerating the overall rate of global warming. Glaciers, sea ice and tundra will melt, contributing to global sea level rises. A warmer Arctic would also diminish the Gulf Stream, which brings warmer water and weather to north-western Europe.

Prediction of weather tomorrow or the climate in 100 years from now requires the knowledge of the circulations in the atmosphere. Weather and climate models convert this knowledge and they then simulate these circulations. Thus, models become very important to the interpretation of future climate development and also dominate the technical basis for the political climate debate. In short, it is vital that these models are as good as possible and work to improve these models is an ongoing process.

In the present work I am using output from Denmark Meteorological Institutes (DMI) Numerical Weather Prediction (NWP) model HIRLAM 7.3, run at a resolution of 5 km and forced with ECMWF global model. To give context to this, a background climatology, calculated using the HIRHAM5 Regional Climate Model (RCM), runs from 1980-2016 at a resolution of 5 km and forced on the boundaries by ERA-Interim was used. Focus is on the SMB component precipitation. This thesis aims to compare model output precipitation for a short overlapping period (2014-2016) where the RCM and NWP model have both been operational, to assess model biases between the climatology and operational data product.

2 Background

2.1 Climate change

Climate change is a change in average weather conditions considered over long periods of time. Climate change is caused by external drivers such as the Milankovitch cycles, solar activity, or human influences along with many more. One of the Milankovitch cycles describe how the Earth orbits around the Sun in an elliptical orbit. From gravitational pull by the other planets in the solar system, comes variations of how much the ellipse depart from circularity. Slight variations in Earth's orbit lead to changes in the seasonal distribution of sunlight reaching the Earth's surface and how it is distributed across the globe. Furthermore, the output of the Sun varies, and this solar variability also influences climate change.

The sunlight travels through the air with little effect upon the air itself. It travels in the form of a wave, and if absorbed by an object this object can later emit energy in the form of radiation. As these waves have both electric and magnetic properties they are called electromagnetic waves. To explain some of these waves behaviour, which are those of a particle, radiation can be considered as streams of particles or discrete packets of energy (photons) (Young et al., 2012). The wavelength of radiation emitted by an object depends primary on the objects temperature. Since inside objects there are billions of rapidly vibrating electrons, from where the energy originates. The higher the temperature, the faster the electrons vibrate, and the shorter the emitted wavelengths are. When the temperature of an object is increasing the total radiation emitted is increasing, this is known as the Stefan Boltzmanns law.

The Stefan Boltzmann law,

$$E = \sigma T^4 [W/m^2] \quad (1)$$

Wien displacement law,

$$\lambda_m T = 2.90 \times 10^{-3} [mK] \quad (2)$$

The Planck–Einstein relation,

$$E = \frac{hc}{\lambda} [J] \quad (3)$$

Where E is the total energy radiated per unit area per unit time, $\sigma = 5.67 \times 10^{-8} \frac{W}{K^4 m^2}$ is the Stefan-Boltzmann constant, and T is the objects surface temperature in Kelvin. This relationship stated that all objects with temperature above absolute zero emit radiation at a rate proportional to the forth power of its absolute temperature. Consequently, a small change in temperature results in a large change in radiation.

An object can only emit radiation at a certain wavelength if it also can absorb radiation at said wavelength. Blackbodies are idealised object that can absorb and emit radiation at all wavelengths/frequencies. The Sun is a good example of a blackbody. The surface temperature of the Sun is close to 5800 K while the Earth's average surface temperature is approximated to 288 K (Ahrens, 2013). Hence, the Sun emits shortwave radiation and the Earth is emitting longwave radiation. In Figure 1 the Earth's Infrared (IR) radiation

as a function of wavelength for various absolute temperatures is depicted. Each curve in Figure 1 is seen to peak at somewhat different wavelength. Wiens displacement law (Equation 2) describes the shift of that peak in terms of temperature.

The papers of this thesis is radiating electromagnetic waves, but as the temperature of the paper only is around 293 K the wavelengths are too small for human vision. The page is visible since other sources light-waves are reflected off the paper, known as the albedo effect. Surface albedo is defined as the ratio of irradiance reflected to the incident irradiance received by a surface. This is measured on a scale from 0.0 to 1.0, from no reflection to all light being reflected respectively. Objects that are good absorbers of radiation are also good emitters of it. A black surface is both a good emitter and a good absorber, while a white object that is highly reflecting absorbs rather little and emits rather little too. Leading to if there is a decrease in ice extent in the Arctic there will be a resulting lower albedo.

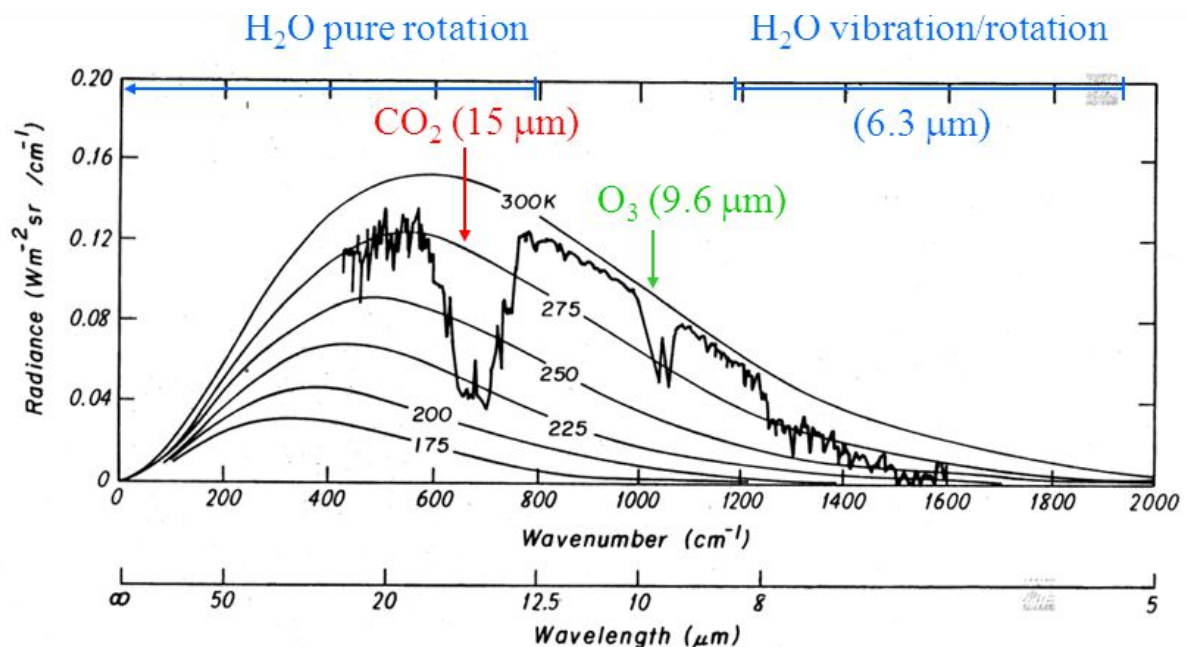


Figure 1: Thermal IR spectrum for Earth. The common greenhouse gases, carbondioxid (red arrow), ozone (green arrow) and water vapor (blue arrows) absorb IR radiation at specific wavelengths. Ref: K-N. Liou, *Radiation and cloud Physics Processes in the Atmosphere* (1992).

Reflection and absorption reduce the radiation at the Earth's surface. Figure 1 shows a radiation spectra over the Earth by combining blackbody spectra of different temperatures. The emitted wavelengths are IR radiation, consisting of wavelengths between 700 nm – 1mm or with frequencies in the range of 430 THz – 300 GHz. Figure 1 shows how IR radiation at certain characteristic frequencies (of the GHGs) is absorbed by the atmosphere. These GHGs will re-emit the radiation at the same frequency, in all directions, but with lower energy when it is higher up in the troposphere, as it gets colder. The IR

radiation is, on average, reflected away from Earth at a greater height, when the concentration of the GHG absorbing and emitting that frequency is low. The atmosphere below this height, to restore radiative convective equilibrium or thermal equilibrium, raises its temperature, trapping heat in the lower atmosphere (Houghton, 2015). The IPCC AR5 also concluded there is a greater than 95 percent probability that human-produced GHGs such as carbon dioxide, methane and nitrous oxide have caused much of the observed increase in Earth's temperatures over the past 50 years.

Ice sheets are considered among one of the most sensitive indicators of climate change and as global average temperatures rises, the ice sheets retreat.

2.2 Greenland ice sheet

In response to global warming of the atmosphere and oceans the global sea level rises. From thermal expansion caused by warming of the ocean (water expands as it warms) and from increased melting of land-based ice, like glaciers and ice sheets. Ice losses from Antarctica and Greenland are the largest source of uncertainty in sea-level projections.

The Arctic as a whole has been warming more than twice as rapidly than the global average for the past 50 years (AMAP, 2017). Same report show that in January 2016 the Arctic was 5°C warmer than the 1981-2010 average for the region, and monthly mean temperatures for October to December was 6°C higher than the averages for these months. Climate models also project increases in autumn and winter season precipitation. If the atmosphere gets warmer, the air can carry more moisture. Consequently, increase in precipitation amount is to be expected. And recent added melt processes affecting Arctic and Antarctic suggest that the low-end projections of sea-level rise made by the Intergovernmental Panel on Climate Change (IPCC) are underestimated (AMAP, 2017).

Greenland is located 72.0000° N and 40.0000° W. The Greenland ice sheet is a vast body of ice covering 1.71 million km², which is approximately 80 % of the entire surface of Greenland. This is the second, after the Antarctica ice sheet, largest ice body in the world. The mean altitude of the Greenland ice sheet is almost 2200 m, with a maximum at close to 3200 m. Hence, the thickness of the ice sheet is broadly more than 2 km, yielding around 2.85 million km³ of ice. That amount is comparable to 7.2 m sea level rise (IPCC, 2013).

2.3 Surface mass balance and dynamic mass loss

At the present day ice caps and glaciers covers a tenth of the Earth's surface (Alean et al., 2016). The SMB consists of a negative and a positive mass term. Ablation, the negative mass term, consists of evaporation, sublimation, and meltwater running off glaciers. Snowfall accumulation on glaciers is a positive mass term and the most common, continuously adding new layers to the surface.

This is balanced by how glaciers flow under gravity from high to low levels and can hence be approximated as a viscous fluid. The equilibrium line, when accumulation equals ablation, is normally located close to the coast at the outermost part of the glacier (see Figure 2). Above the equilibrium line is the accumulation zone, where more mass is gained than lost. Below the equilibrium line the net mass loss exceeds accumulation. This make up the SMB.

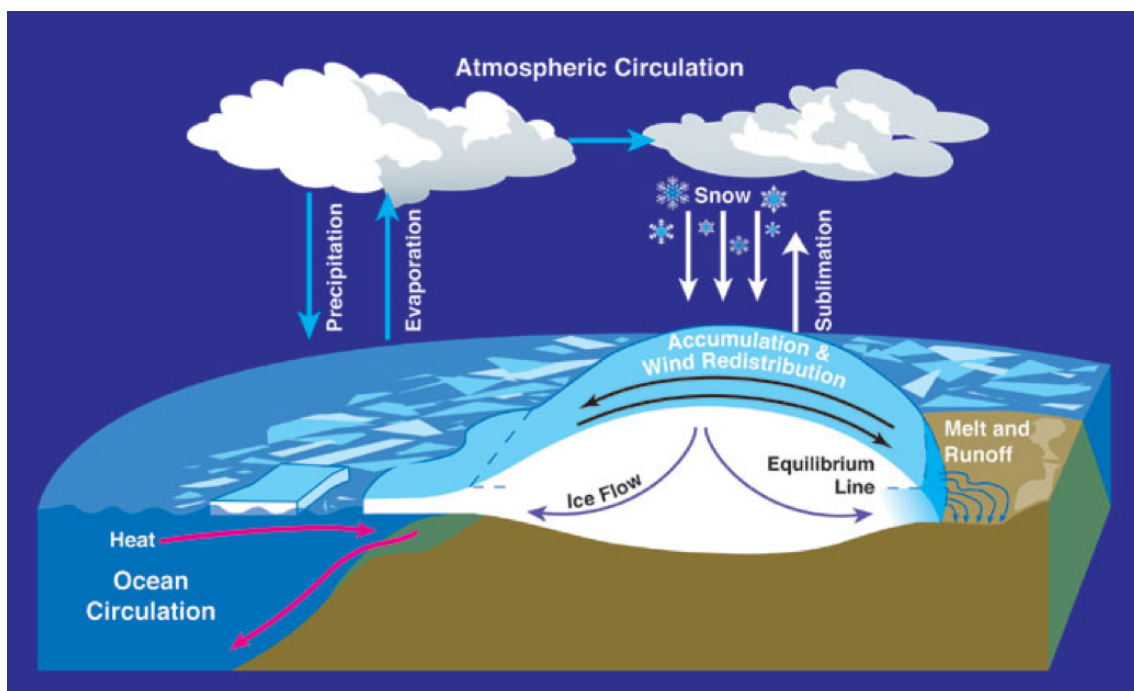


Figure 2: Illustrating glacier mass balance and atmospheric circulations. Ref: NASA.gov

Surface Mass Balance = Accumulation – Ablation

Accumulation = snowfall + condensation + refreezing

Ablation = Melt(runoff) + sublimation

Surface budget (SMB) + dynamic budget = Total mass budget

The total mass budget also includes important dynamical processes such as ice berg calving (Shepard et al., 2012). Ice berg calving is when a large block of ice breaks off the ice sheet and crashes into the water. As much as one third of mass loss is attributed to iceberg calving in Greenland (Enderlin et al., 2014). Results from gravimetry satellites indicate a negative mass budget, with around -234 ± 20 Gt of net mass (Baretta et al., 2013) being lost each year. Iceberg calving and submarine melt are important mass loss processes, it is believed to account for around 30-40% of mass loss from Greenland and close to 80% in Antarctica.

2.4 Climate and weather models

Weather and climate are two sides of the same coin, since climate can be defined as the average weather over a longer time scale. To describe the weather at a given location is not that hard, it only requires the knowledge of temperature, pressure, humidity and wind direction. However, it is considerably harder to *predict* the weather. Even though we through history have made great efforts to be able to produce more accurate weather forecasts and with todays numerous data from monitoring stations and enormous processing power at our disposal, it is still not possible to make reliable weather forecasts that stretches further than a week into the future.

The foundation of a climate model is the laws of physics and these laws can be expressed quantitatively by mathematical equations. The idea is that if we know todays atmospheric conditions, we can use these equations to integrate known parameters over time. The chaotic nature of the climate system and the equations that describe it, results in that the equations become more inaccurate the further we try to look into the future. While this is a more pressing problem for weather forecasts it is less important for climate scientist who are interested in the average weather over a long period of time. This average, which we call the *climate*, is essentially determined by boundary conditions such as the CO_2 content in the atmosphere and solar radiation mentioned in the section on climate change 2.1.

The most important laws of physics which are incorporated in climate models are:

- The Navier Stokes equations, based on Newtons laws, describe the forces that act on an air parcel in a three-dimensional rotating system, describe the conservation of momentum,

$$\frac{Du}{Dt} = \frac{uv \tan \phi}{a} - \frac{uw}{a} - \frac{1}{\rho} \frac{\partial P}{\partial x} + 2\Omega v \sin \Phi - 2\Omega \cos \phi + F_{rx} \quad (4)$$

$$\frac{Dv}{Dt} = \frac{-u^2 \tan \phi}{a} - \frac{vw}{a} - \frac{1}{\rho} \frac{\partial P}{\partial y} - 2\Omega \sin \Phi + F_{ry} \quad (5)$$

$$\frac{Dw}{Dt} = \frac{u^2 + v^2}{a} - \frac{1}{\rho} \frac{\partial P}{\partial z} - g + 2\Omega \cos \Phi + F_{rz} \quad (6)$$

- Conservation of mass applied to the atmosphere, equation of continuity,

$$\frac{\partial u}{\partial x} + \frac{\partial v}{\partial y} + \frac{\partial w}{\partial z} = 0 \quad (7)$$

- Conservation of energy, the equation for first law of thermodynamics,

$$DQ = C_p DT - \left(\frac{1}{\rho}\right) Dp \quad (8)$$

- Equation of the state of ideal gases,

$$PV = nRT \quad (9)$$

- Radiation equations describing how solar and thermal radiation is propagated and converted in the atmosphere (see background section climate change equations 1,2,3).

Complementing the laws of physics are empirical laws, relationships based mostly on observations and does not necessarily have a theoretical basis. The key feature for such empirical laws are to describe processes in time and space scales beyond the models resolution. An example are gravity waves; an air mass that is in equilibrium with its surroundings moves vertically into an area of a different density and then the Earth's gravitational field pulls the air mass back to the point of origin. Resulting in a oscillation around the equilibrium point. As these waves have a shorter wavelength than the models resolution they are described by a set of equations based on observations and theoretical considerations. Or the effects from topography and land representation in different models. A key process in cloud formation and precipitation is rising air. A parcel of air expands as it rises and this expansion, or work, causes the temperature of the air parcel to decrease. As the parcel rises, the relative humidity increases until it reaches 100 %. When this occurs, excess water vapor condenses on aerosol particles, forming clouds. Above this point the cloud droplets grow by condensation in the rising air and if the cloud is sufficiently deep or long lived, precipitation will develop (Holton et al., 2013).

3 Method

3.1 HIRLAM 7.3 - Regional weather prediction model

HIRLAM 7.3, the High Resolution Limited Area Model, is a numerical Weather Prediction (NWP) forecast system developed and continuously upgraded by the international HIRLAM programme. The member institutes are the National Meteorological Services in Denmark, Finland, Iceland, Ireland, Netherlands, Norway, Spain and Sweden.

The HIRLAM 7.3 model is a hydrostatic grid-point model, on which the dynamical core is based on a semi-Lagrangian (following the motion) discretisation of the multi-level primitive equations (See equations 4-9). Optionally, a Eulerian (fixed point coordinate system) scheme can be used as well. The model was run on a 5-km resolution in the horizontal and with 65 vertical levels for the atmosphere, forced at the boundaries by the European Centre for Medium-Range Weather Forecasts (ECMWF) hi-resolution global model, EC-HRES – a 9km resolution model. The prognostic variables horizontal wind components u, v , temperature T , specific humidity q are defined at each levels in the model. When pressure p , geopotential height ϕ and vertical wind velocity are calculated at half levels. These equations are adopted onto a lat-lon rotated grid. The HIRLAM model physical parameterisation includes a tiled surface scheme a turbulence parameterisation a radiation scheme and a gravity wave drag parameterisation. The main new feature of this compared with HIRLAM 7.2 is the surface scheme physics implementation (Gollvik, 2010). The new surface scheme, newsnow, provides a tiled surface scheme (Gollvik, 2010). The latest radiation scheme allows the model to handle clouds with different sizes of cloud droplets and ice crystals in a more realistic manner. Using that the size of the droplet mainly affects the short-wave radiation of thin clouds. For the most part, the water clouds are represented as slightly less and the ice clouds are represented as slightly more transparent than the original radiation scheme (Whyser et al., 1999; Rontu et al., 2017).

3.2 HIRHAM5 - Regional climate model

The High Resolution Hamburg Climate Model 5 is a RCM that requires three sets of input files: boundary files, climatology files and sea surface temperature files. HIRHAM5 combines the dynamical core from the HIRLAM7.3 NWP model with the physics schemes and parameterisation from the atmospheric chemistry general circulation model (global climate model) ECHAM5 (Roeckner et al., 2003). In all off the Greenland domain HIRHAM5 Is run on a horizontal 0.05×0.05 rotated-pole grid translated to approximately a resolution of 5,5 km. The Atmosphere has 31 levels in the vertical. At the boundaries, the HIRHAM5 model is driven by ERA-Interim reanalysis a 75km resolution model (Dee et al, 2011) providing atmospheric model-level fields of temperature and humidity as well as wind and surface pressure. ERA-Interim, a global atmospheric reanalysis from 1979 and continuously updated in real time is produced by the ECMWF. The ERAI product yields output every three hours for surface parameters, along with weather condition for both land-surface and ocean. Upper-air parameters data for the stratosphere and the

troposphere is attained every six hour. Thus, the HIRHAM5 model gets forced every six hour on the boundaries with a daily sea surface temperature. The function of reanalysis is to yield a homogeneous record of past atmospheric evolution.

3.3 Data analysis

Data was analysed with the Climate Data Operators (CDO) and MATLAB software. CDO is a large tool set for working on climate and NWP model data. CDO software is a collection of multiple command line operators for manipulating and analysing of climate and forecast model data. It provides more than 600 operators for this purpose, and it has a small memory requirement that enables CDOs to process very large files, larger than the physical memory of the software itself. The development of CDO was designed to have the same set of processing functions for both GRIB (Gridded Binary or General Regularly-distributed Information in Binary form) and NetCDF (Network Common Data Form) datasets. GRIB is a data format often used in meteorology for storage of past weather data, and for storage of weather forecast data. GRIB data file format is used by the World Meteorological Organization (WMO). Converted GRIB model data output into NetCDF allowing for the usage of better software tools. NetCDF is a set of interfaces for array-oriented data for representing scientific data. A wide range of application software has been made which make use of NetCDF files. The commonly used Linux/Unix command line utilities were used in this study.

4 Result and Discussion

4.1 Model output of precipitation

The progression of this thesis work is shown in this section with selected figures for observation. Firstly, displaying the parameters which are the focus of this study, followed by an investigation of the parameters. The SMB model is based partly on observations on the ice sheet from automatic weather stations, and partly on DMI's high resolution NWP model HIRLAM 7.3 and the RCM HIRHAM5. Total precipitation, rainfall and snowfall were selected to study since accumulation on the Greenland ice sheets most important component is precipitation. As precipitation is a vital part for calculating the SMB, knowledge of potential biases between the models used to provide the data for the SMB model are necessary. The chosen parameters for evaluation revealed differences between the two models and these are illustrated in diagrams and maps together with a special case study in section 4.2. For all processed data, an ice sheet mask was used. The ice sheet mask simply cuts away all the data outside the domain of the ice sheet as we are only focusing on the effects on the ice sheet and not around it.

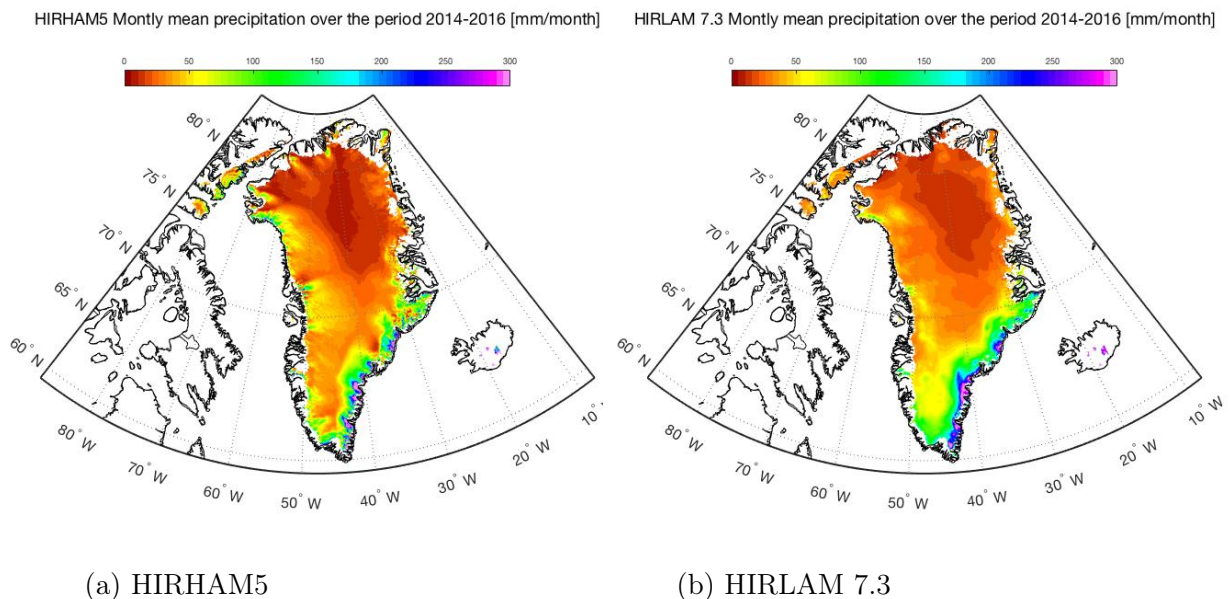


Figure 3: Simulated model output of monthly mean total precipitation [mm/month] during the period 2014-2016 over the Greenland ice sheet. From HIRHAM5 in (a), from HIRLAM 7.3 in (b).

This study was done for a short overlapping period between 2014-2016, when both of the two models were operational. By plotting the monthly mean total precipitation for the period 2014 to 2016 a basis outlook on average amount and location occurrence of precipitation on the Greenland ice sheet was obtained. This is depicted in Figure 3a from HIRHAM5 and Figure 3b from HIRLAM 7.3. Noticeable differences between the models were observed on a few locations. One significant area was the southeast-coast of the Greenland ice sheet. This is visible in figure 3, as the blue and purple band along

the coastline in 3b illustrate a wide band of considerable amount of precipitation, for HIRLAM 7.3. Compare with HIRHAM5 displayed in 3b were a more local distribution is simulated, depicted as blue and purple spots along the coastline. This was also further investigated in section 4.2.

Figure 4 illustrates the difference between the two models, HIRHAM5 and HIRLAM 7.3, simulated output in Figure 3. The red colour scale indicated that a larger amount of monthly mean precipitation was simulated in HIRHAM5. The blue colour scale argue that a larger amount was being simulated in HIRLAM 7.3. From the overrepresentation of blue in Figure 4 it can be distinguished that the NWP model HIRLAM 7.3 was a wetter model than the RCM HIRHAM5 over the Greenland ice sheet for this investigated time period. Another observation is made along the ice sheet mask edge, note the local red spots visual close to the southeast-coastline of Greenland. These are implying HIRHAM5 were simulating a more sizeable amount of average precipitation locally. An example of this is at 38.0000° W and 66.5000° N, well visible in both Figure 3 and 4. The results from this study propose that HIRLAM 7.3 on average simulate more precipitation over the Greenland ice sheet than HIRHAM5. These results were not expected, in fact the hypothesis was that it was the other way around.

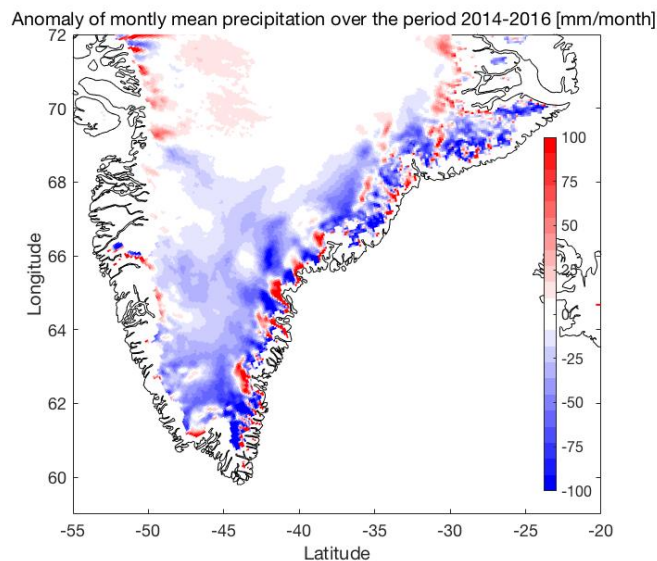


Figure 4: Anomaly between HIRHAM5 and HIRLAM 7.3, for model output of monthly mean precipitation during the period 2014-2016 in [mm/month] of the southeast Greenland ice sheet. Red indicated larger amount of total precipitation simulated in HIRHAM5 compared with HIRLAM 7.3. Blue illustrate more total precipitation simulated by HIRLAM 7.3 compared with HIRHAM5 in that area.

One reason for these differences in precipitation we see in Figure 4 could be the subgrid-scale orography (mountain like terrain), which occurs at length-scales that cannot be adequately resolves on the computational mesh. Orography is a physiographic field that in the models are specialised for the study of topographic regions of elevated terrain, like in mountain areas or like on the Greenland ice sheet. If the two models have significant

differences between their orographic parameterisation consequently the topography of the two models would not match at all points, then a distinction between the models simulated precipitation seems authentic. Accordingly, the parameterisation of orographic gravity waves explained in section 2.4 then differ between the models, which would conjecture differences in precipitation patterns from forced ascent of air reaching saturation. The red spots along the southeast- coast of the Greenland ice sheet illustrating higher amount of precipitation from HIRHAM5 compared with HIRLAM 7.3 could be explained by a difference between orographic parameterisation. This is further investigated in section 4.3.

4.2 Extreme precipitation event October 2016

As a result of climate change, more severe weather events are expected in the future, as warmer air can carry more moisture. Severe weather events that unloads more amount of precipitation on the Greenland ice sheet will add more mass to the surface. In 2015 the SMB was at 50 Gt mass gain while the year after, 2016, had 550 Gt mass gained. In the Appendix figures of seasonal average precipitation for the entire investigated period is listed. Over the year, it snows more than it melts, but calving of icebergs is also part of the total mass budget of the ice sheet. If the ice sheet was in balance, the calving should match this net accumulation over the year. Satellite observations over the past decade show, however, that the ice sheet is not in balance. The calving loss is greater than the gain from surface mass balance. For the past decades, the net mass loss of the ice sheet has been more than 200 Gt annually. The high surface mass gain in 2016 compared with that in 2015 was due to extreme weather events and 2016 came close to a total mass budget of zero.

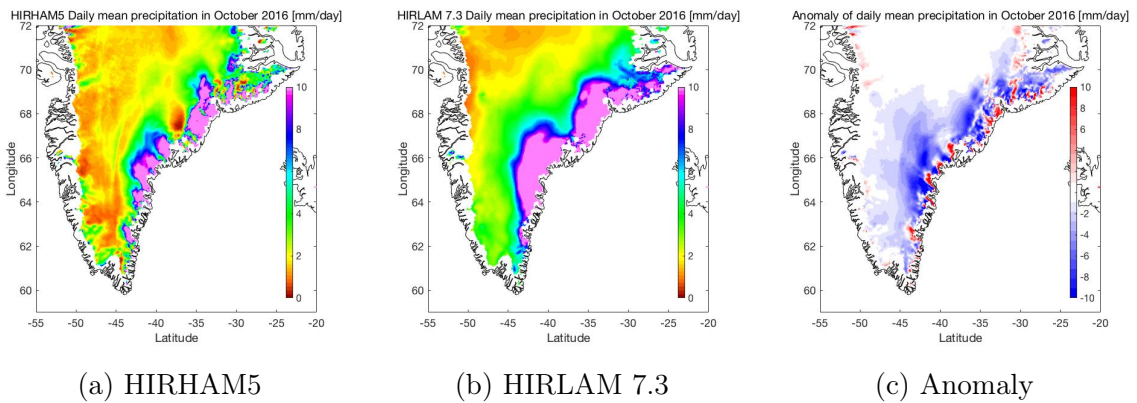


Figure 5: Simulated model output of daily mean total precipitation [mm/day] over the southeast Greenland ice sheet for October 2016. From HIRHAM5 in (a), from HIRLAM 7.3 in (b), and the anomaly of (a) minus (b) in (c).

In October 2016, atmospheric rivers, horizontal transport regions of water vapor, associated with former hurricanes Nicole and Matthew led to extreme precipitation in Greenland. This case study was created to observe the daily data sets of accumulation and the partition between snowfall and rainfall. The amount of precipitation as a percent-

age is significantly higher for this case study compared with the average precipitation (1981-2010) from the EC-HRES model. Figure 5 show the simulated daily average total precipitation in October 2016 in mm/day. In Figures 3-5 the same precipitation patterns are shown, affirming that most amount of precipitation is falling on the southeast side of Greenland. This is a characteristic pattern seen in other studies and other model outputs for Greenland. The trade winds generally come from southwest, the westerlies. Cyclones follow the track of the westerlies, and this is explaining the high concentration of precipitation on the southeast-coast of Greenland.

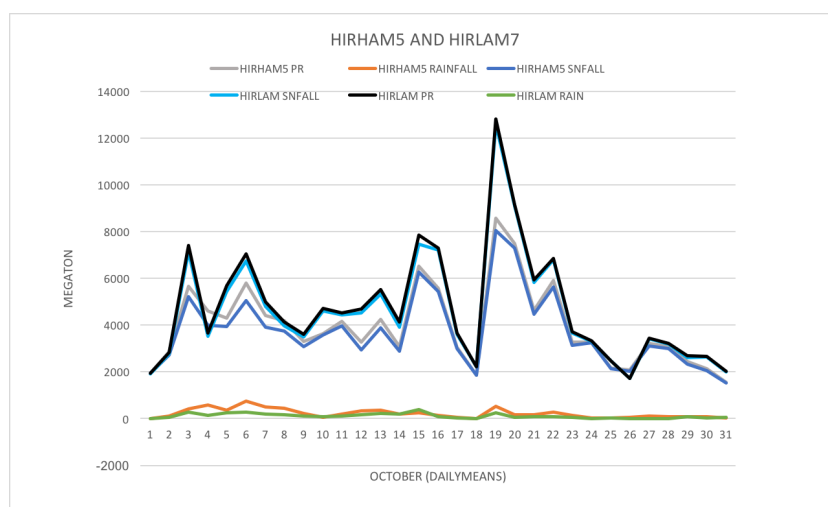


Figure 6: Detailed total precipitation, snowfall and rainfall in [Mt/day] for HIRHAM5 and HIRLAM 7.3 during October 2016

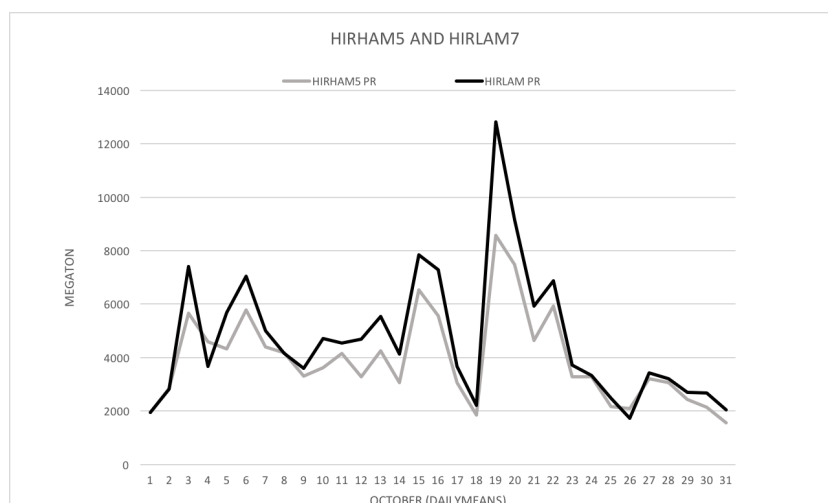


Figure 7: Total precipitation [Mt/day] for HIRHAM5 and HIRLAM 7.3 in October 2016

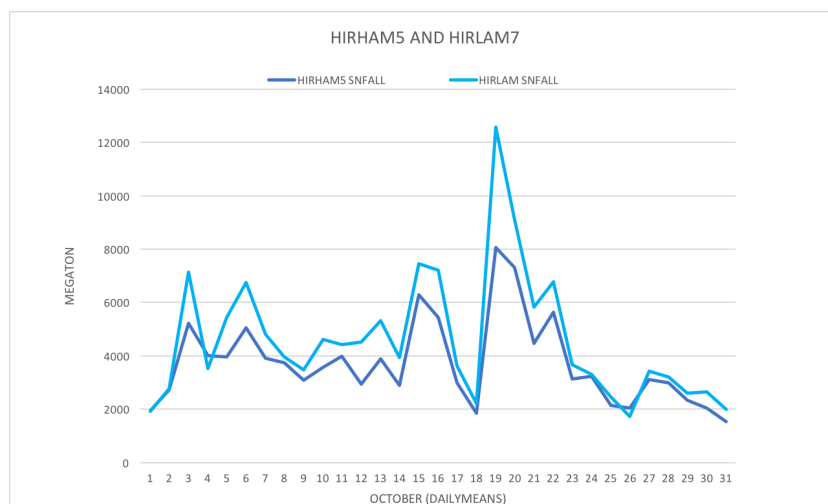


Figure 8: Snowfall [Mt/day] for HIRHAM5 and HIRLAM 7.3 in October 2016

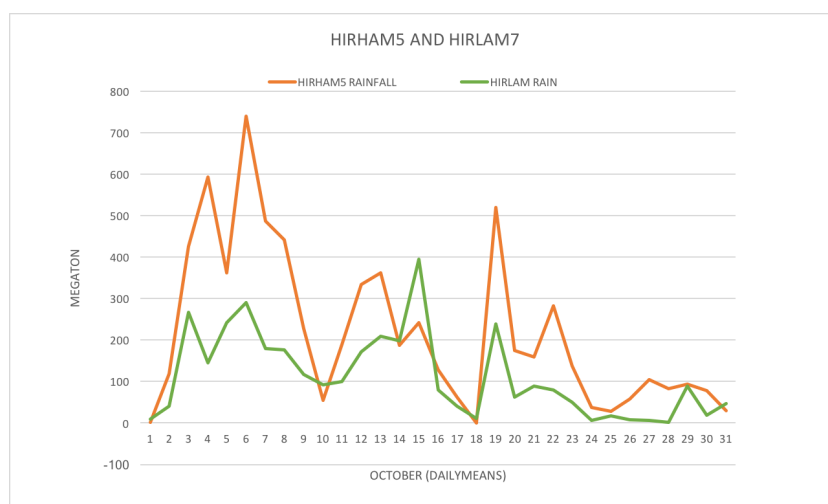


Figure 9: Rainfall [Mt/day] for HIRHAM5 and HIRLAM 7.3 in October 2016

SMB is calculated in units of ton, t, ergo the units for total precipitation, snowfall and rainfall are converted to Megaton, Mt, in figures 6-9. Figure 6 shows daily mean values of total precipitation along with snowfall and rainfall for the two different models. The correlation between the two models are seen in Figure 6, as peaks and sinks have a nice consistency throughout the diagram. The same pattern similarities are found throughout the period between 2014-2016. This agree with a minuscule time delay between the two models. A more sizable delay would be explained briefly as when a model unloads the same amount of precipitation but at slightly shifted simulated model locations. Then an offset between the two models should have been prominent in a diagram. But this is not the case in this study.

Figures 7-9 show the relation between the three parameters, total precipitation, snowfall, and rainfall respectively. Once more it is shown how HIRLAM 7.3 simulate a larger amount of total precipitation than HIRHAM5. This is likewise the result in Figure 8 were snowfall amounts in HIRLAM 7.3 exceed the amount of snowfall simulated by HIRHAM5.

In Figure 9 the orange line represents rainfall simulated by the RCM HIRHAM5 and the green line serve as representation for simulated rainfall by the NWP model HIRLAM 7.3. Firstly, between the 10th of October to the 17th of October we see this time difference explained in the paragraph above between the two models. These are well documented dates, in reality a substantial amount of precipitation fell over the Greenland ice sheet on the 15th of October 2016. Apart from the example just described, there is a nice correlation between the model output for rainfall. In the previous example discussing Figure 6 HIRLAM 7.3 simulated higher amounts of precipitation than HIRHAM5, in Figure 9 it is the reverse. HIRHAM5 is for October 2016 simulating larger amounts of rainfall than HIRLAM 7.3. This would be relevant for operational meteorology but it is not significant for climate modelling on Greenland, as model output of rainfall compared with snowfall make an infinitesimal effect on the SMB budget.

The difference of rain and snow between the models put forward for consideration that one possible reason could be that the cloud schemes used in the two models are not the same. Further studies are needed.

In the method, section 3.1, a key new feature of the radiation scheme used in HIRLAM 7.3 is mentioned. This feature explained how low clouds, consisting of water droplets, are slightly less transparent than high clouds built of ice crystals. Water clouds compared with ice clouds reflect more shortwave radiation resulting in cooling the surface of the Earth. While high thin clouds primarily transmit incoming solar radiation, and at the same time trap some of the outgoing longwave radiation emitted by the Earth and radiate it back downward. Ergo, warming the surface of the Earth.

A more realistic radiation scheme would implement a better cloud scheme, and could suggest that HIRLAM 7.3 were the more realistic model for precipitation simulations on the Greenland ice sheet done in this study. Evaluating the model output with observations from automatic weather stations would be needed to be able to make such a claim. Unfortunately, harsh conditions on the Greenland ice sheet makes it hard to make reliable measurements. This is especially true for precipitation. One way such measurements are collected is by height measurements. As the snow fall the surface it lands on is elevated. From winds this is a major uncertainty and no reliable data was available during the duration of this study.

4.3 Topography

Figure 10a illustrate the topography on the ice sheet used in RCM HIRHAM5, and Figure 10b display the topography of the ice sheet used in the NWP model HIRLAM 7.3. The units were set in meters and ranged from 0 m up to 3000 m on account of the maximum elevation of the Greenland ice sheet being close to 3200 m high. There were obvious differences between the models. The example discussed in section 4.1 at 38.0000° W and 66.5000° N, where HIRHAM5 simulated higher amount of precipitation and which were well visible in both Figure 3,4 and 5 shows a topographic difference in Figure 10. Concerning the example at 38.0000° W and 66.5000° N, in Figure 10a a larger area of elevation above 3000 m was depicted than in Figure 10b. For this case, HIRHAM5 had more elevated topography than HIRLAM 7.3. It might be from orographic lift that HIRHAM5 were simulating more precipitation in this area than HIRLAM 7.3.

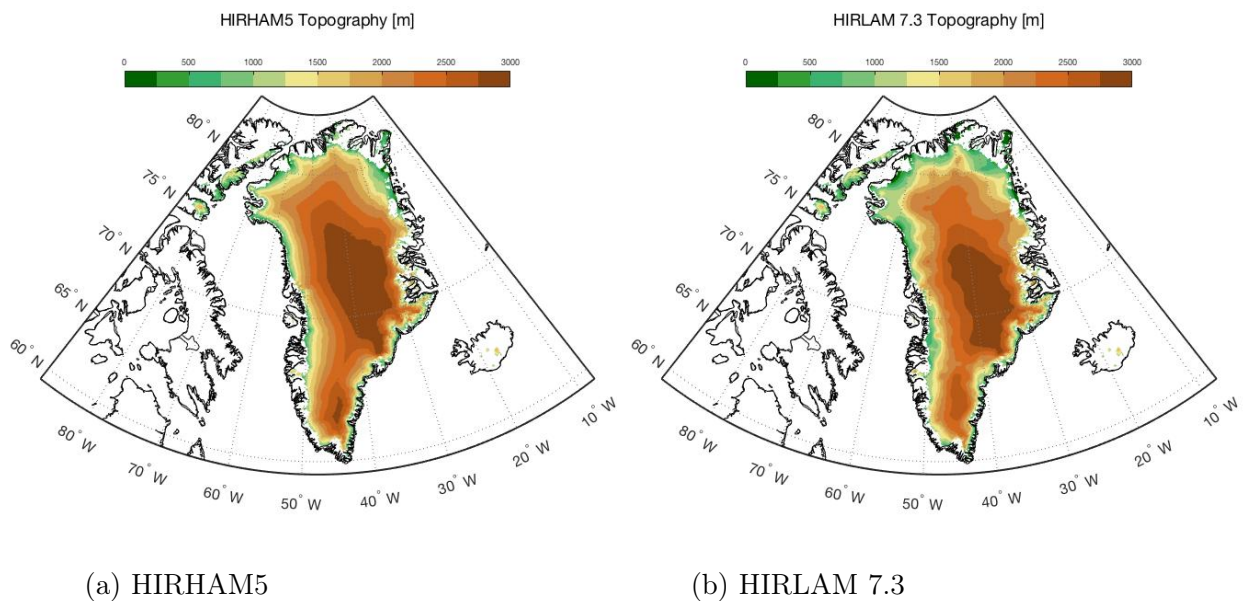


Figure 10: Topography [m] over the Greenland ice sheet for the two models. HIRHAM5 in (a), and HIRLAM 7.3 in (b).

The contour lines of the topography in HIRHAM5 had an overall appearance being straighter than those of HIRLAM 7.3 with a more curved presentation. Concerning the northern part of Greenland one difference easy to identify are the spots in Figure 10b, one was found at 40.0000° W 81.0000° N. Another at 50.0000° W 78.0000° N. In Figure 11 a contour plotting done in MATLAB make these spots became apparent along with several more distributed over the ice sheet. The spots in HIRLAM 7.3 surface look very much like an interpolation artefact known as “bull’s-eye” pattern. Interpolation is when you create a continuous surface from a set of points. The pattern seen in Figure 11 correlates to when interpolating between data points that are heterogeneously spaced, that is with clusters of points that are widely spaced over the whole domain.

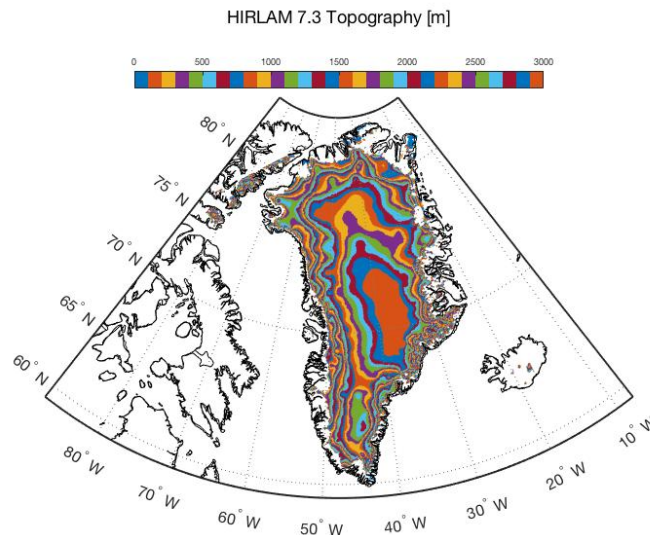


Figure 11: Topography [m] over the Greenland ice sheet from HIRLAM 7.3

In Figure 12 the difference between the topography used in HIRHAM5 and HIRLAM 7.3 are exposed, for the entire domain used in this study and for the south of Greenland. In northwest part of Greenland HIRHAM5 has a higher elevation, the red curve between 75.0000° N and 80.0000° N, that consists well with the curved contours of HIRLAM 7.3 topography seen in Figure 11. This shows how HIRLAM 7.3 has a lower elevation of the surface compared to HIRHAM5 corresponding to the red curve in Figure 12. At 38.0000° W and 66.5000° N, at which HIRHAM5 model output simulated more precipitation than HIRLAM 7.3, Figure 12 display a heightened topography at that location for HIRHAM5. This argument is not consistent throughout the entire studied domain. Following the southeast-coast of the Greenland ice sheet blue spots indicate a more elevated surface in HIRLAM 7.3 occur at equal locations of areas of more precipitation simulated by HIRHAM5 (see figure 12 and 4). An example off this is the red line in Figure 4 and the blue line in figure 12 at 44.000° W and 63.0000° N.

The differences in precipitation patterns between the two models can with some confidence be partly ascribed to different topographies, especially in the north of Greenland.

HIRHAM5 has a better surface scheme over ice points, like all climate models it needs to be able to simulate what is happening over a long period at the surface. HIRLAM 7.3 has not been much developed for ice surfaces. Hence, it is expected that the topography is more realistic in HIRHAM5 – it uses a DEM created in 2001. HIRLAM 7.3 topography has not been updated since the 1990s.

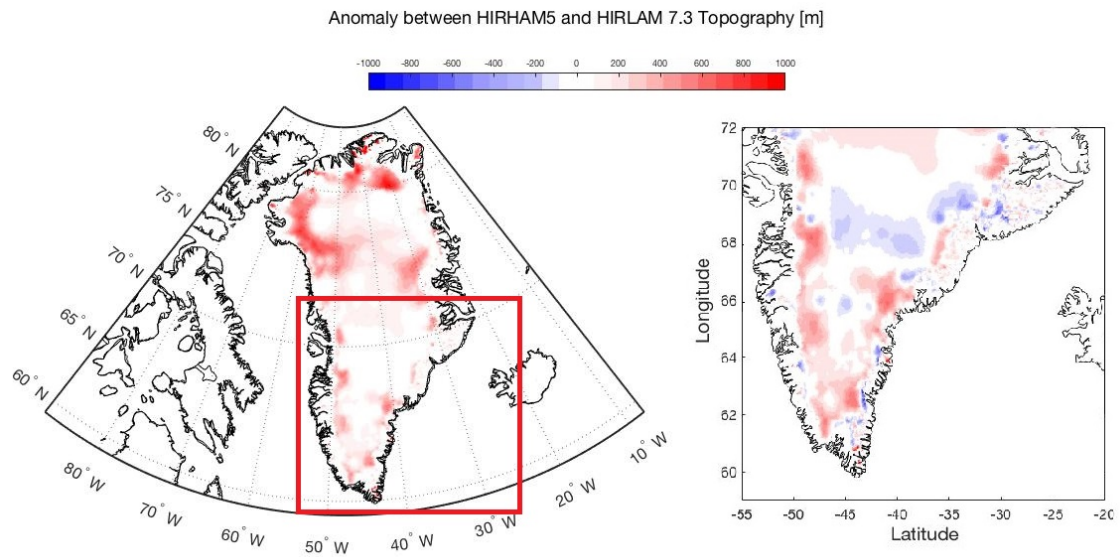


Figure 12: Anomaly between the two models topography [m], where red imply HIRHAM5 has a more elevated surface at that area. Blue express HIRLAM 7.3 have a higher surface compared with HIRHAM5 in that area.

5 Conclusions and Outlook

In the present work of this thesis the high-resolution models HIRHAM5 and HIRLAM 7.3 used in SMB calculations were compared to assess model biases. This study is done over an overlapping period, 2014-2016, when both models have been operational. HIRLAM 7.3 model outputs revealed higher amount of simulated precipitation over the entire domain compared with HIRHAM5 that were simulating a higher amount of average precipitation locally along the edges of the ice sheet. The results from this study propose that HIRLAM 7.3 on average simulate more precipitation over the Greenland ice sheet than HIRHAM5. Climate change bring more severe weather events to Greenland, a special case study, primarily on the patrician between snowfall and rainfall, were conducted for such events in October 2016. The correlation of time and placement of precipitation falling on the ice sheet between the two models were nicely consistent throughout the studied period. HIRLAM 7.3 simulated higher amounts of snowfall than HIRHAM5. While HIRHAM5 simulated higher amounts of rainfall than HIRLAM 7.3.

The difference of rainfall and snowfall between the two models seen in this study, put forward for consideration that one reason for this difference could be from that the cloud schemes used in the two models are too different. Another reason for the bias could come from the radiation scheme. Further studies are needed. Next step would be further evaluation between the two models of all parameters used in the SMB model, that should be able to determine whether or not this is of importance for the SMB model calculations. The topography used in HIRLAM 7.3 declare what seems to be an interpolation artefact known as “bull’s-eye” pattern. The differences in precipitation patterns between the two models can with some confidence be partly ascribed to different topographies, especially in the north of Greenland. I suggest comparing these results with observational data, to serve as guidance for future development of these models.

6 Bibliography

Ahrens, C. *Meteorology today*. 10th ed. BROOKS/COLE, pp.31-55.

AMAP, 2017. Adaptation Actions for a Changing Arctic: Perspectives from the Barents Area. Arctic Monitoring and Assessment Programme (AMAP), Oslo, Norway. xiv + 267pp

Alean J, Hambrey M. Glaciers online; 2008. http://www.swisseduc.ch/glaciers/earth_icy_planet/glaciers00-en.html, Accessed: 1st February 2016

Barletta, V. R., L. S. Sørensen, and R. Forsberg (2013) Scatter of mass changes estimates at basin scale for Greenland and Antarctica. *Cryosphere*, 7, 1411-1432, doi: 10.5194/tc-7-1411-2013.

Box, Jason & Fettweis, Xavier & Stroeve, J.C. & Tedesco, Marco & K. Hall, D & Steffen, Konrad. (2012). Greenland Ice Sheet albedo feedback: thermodynamics and atmospheric drivers. *Cryosphere*. 6. 821-831. doi:10.5194/tc-6-821-2012.

Dee, D. P., Uppala, S. M., Simmons, A. J., Berrisford, P., Poli, P., Kobayashi, S., Andrae, U., Balmaseda, M. A., Balsamo, G., Bauer, P., Bechtold, P., Beljaars, A. C. M., van de Berg, L., Bidlot, J., Bormann, N., Delsol, C., Dragani, R., Fuentes, M., Geer, A. J., Haimberger, L., Healy, S. B., Hersbach, H., Hólm, E. V., Isaksen, L., Källberg, P., Köhler, M., Matricardi, M., McNally, A. P., Monge-Sanz, B. M., Morcrette, J.-J., Park, B.-K., Peubey, C., de Rosnay, P., Tavolato, C., Thépaut, J.-N. and Vitart, F. (2011), The ERA-Interim reanalysis: configuration and performance of the data assimilation system. *Q.J.R. Meteorol. Soc.*, 137: 553–597. doi:10.1002/qj.828

Doyle, S. H., A. Hubbard, R. S. W. van de Wal, J. E. Box, D. van As, K. Scharrer, T. W. Meierbachtol, P. C. J. P. Smeets, J. T. Harper, E. Johansson, R. H. Mottram, A. B. Mikkelsen, F. Wilhelms, H. Patton, P. Christoffersen, and B. Hubbard (2015) Amplified melt and flow of the Greenland ice sheet driven by late-summer cyclonic rainfall. *Nat. Geosci.*, 8, 647-653, doi: 10.1038/ngeo2482

Enderlin, E., I. Howat, S. Jeong, M. Noh, J. van Angelen, and M. van den Broeke (2014), An improved mass budget for the Greenland Ice Sheet, *Geophys. Res. Lett.*, 41, 866–872. doi:10.1002/2013GL059010

Freedman, Y., 2012. *University Physics*. 13th ed. San Francisco: Pearson. 1286-1318

Gollvik, S. Samuelsson, P. (2010), A tiled land-surface scheme for HIRLAM. Swedish Meteorological and Hydrological Institute SE-601 76 Norrköping, Sweden., 1-27.

Hanna, E., F. J. Navarro, F. Pattyn, C. M. Domingues, X. Fettweis, E. R. Ivins, R. J. Nicholls, C. Ritz, B. Smith, S. Tulaczyk, P. L. Whitehouse, and H. J. Zwally (2013) Ice-sheet mass balance and climate change. *Nature*, 498, 51-59. doi:10.1038/nature12238

Holton, J., 2013. *Dynamic Meteorology*. 5th ed. Oxford: ACADEMIC PRESS. 1-532

Houghton, J., 2015. *Global warming - the complete briefing*. 5th ed. Cambridge, United Kingdom: Cambridge University Press. 1-396

IPCC (2013) Climate Change 2013: The Physical Science Basis. Contribution of Working Group I to the Fifth Assessment Report of the Intergovernmental Panel on Climate Change (Eds. T. F. Stocker, D. Qin, G.-K. Plattner, M. Tignor, S. K. Allen, J. Boschung, A. Nauels, Y. Xia, V. Bex, and P. M. Midgley). Cambridge University Press, Cambridge, United Kingdom and New York, NY, USA.

Mitchell, J. (2013). An Observational Study of Pack Ice Drift from Atmospheric and Oceanic Momentum Fluxes in the Arctic. *Earth and Environment*. 99, pp 139, ISSN: 1744- 2893

Roeckner, E & Bäuml, G & Bonaventura, Luca & Brokopf, R & Esch, M & Giorgetta, Marco & Hagemann, Stefan & Kirchner, Ingo & Kornblueh, Luis & Manzini, Elisa & Rhodin, A & Schlese, U & Schulzweida, Uwe & Tompkins, A. (2003). The atmospheric general circulation model ECHAM 5. PART I: model description. Max Planck Institute for Meteorology Report. 349. .

Rontu, Laura & Gleeson, Emily & Räisänen, Petri & Nielsen, Kristian & Savijärvi, Hannu & Hansen Sass, Bent. (2017). The HIRLAM fast radiation scheme for mesoscale numerical weather prediction models. *Advances in Science and Research*. 14. 195-215.

Shepherd, A., Ivins, E. R., A, G., Barletta, V. R., Bentley, M. J., Bettadpur, S., Briggs, K. H., Bromwich, D. H., Forsberg, R., Galin, N., Horwath, M., Jacobs, S., Joughin, I., King, M. A., Lenaerts, J. T. M., Li, J., Ligtenberg, S. R. M., Luckman, A., Luthcke, S. B. et al., 2012, 'A reconciled estimate of ice-sheet mass balance', *Science* 338(6111), 1183–1189 (DOI: 10.1126/science.1228102).

Tedesco M, Fettweis X, Mote T, Wahr J, Alexander P, Box JE, Wouters B. Evidence and analysis of 2012 Greenland records from spaceborne observations, a regional climate model and reanalysis data. *Cryosphere*. 2013;7:615–630. doi: 10.5194/tc-7-615-2013.

Wyser, K & Rontu, Laura & Savijärvi, H. (1999). Introducing the effective radius into a fast radiation scheme of a mesoscale model. *Contributions to Atmospheric Physics*. 72. 205-218.

Figure references

K.N: Liou, *Radiation and cloud Physics Processes in the Atmosphere* (1992). Oxford University Press, New York

National Aeronautics and Space Administration. Atmospheric circulation; 2017. http://www.nasa.gov/images/content/53743main_atmos_circ.jpg, Accessed: 12th October 2017.

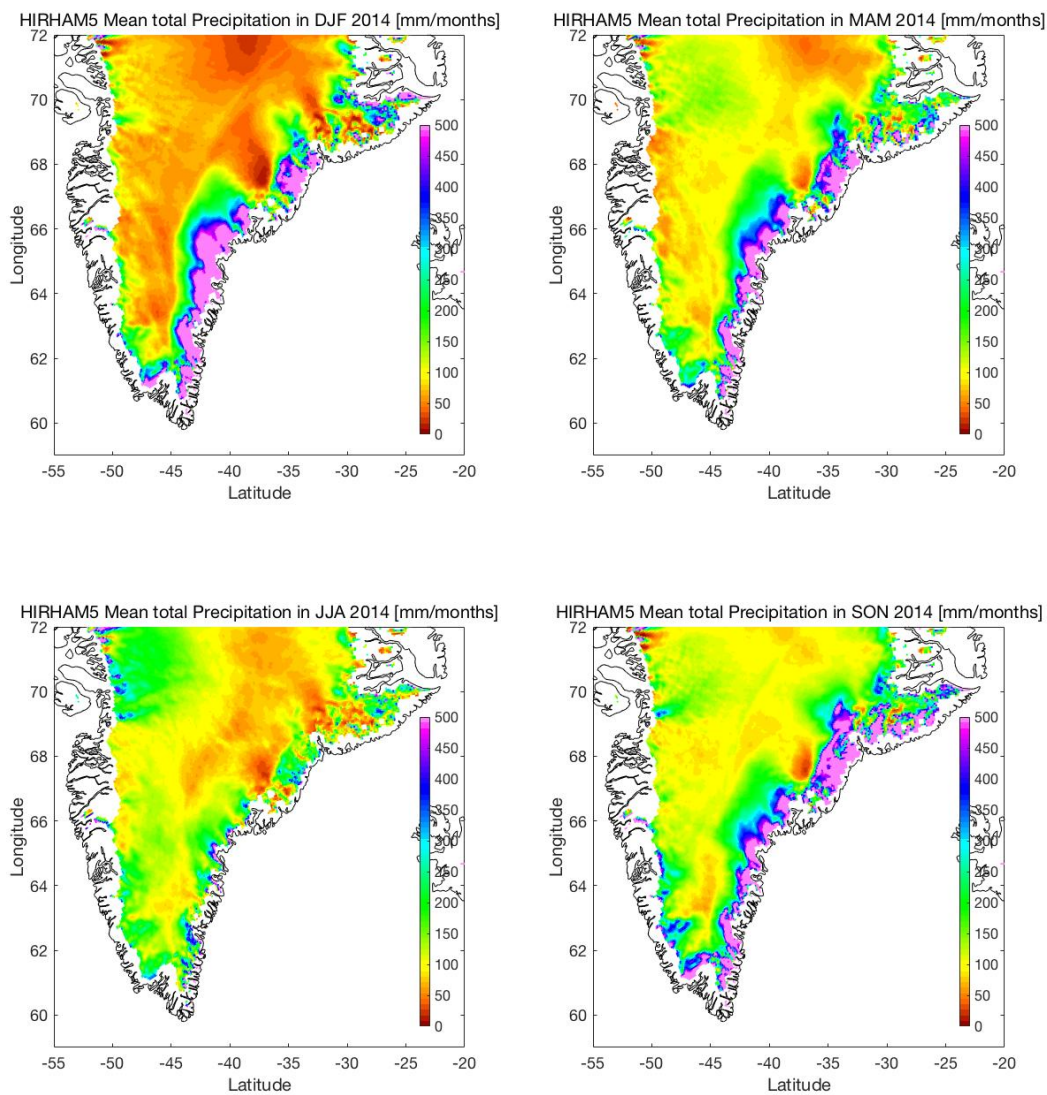
DMI logo. Accessed December 3rd 2017 at <http://www.dmi.dk/om-dmi/presse/dmis-logo/>

Lund university logo. Accessed December 3rd 2017 at <http://www.medarbetarwebben.lu.se/>

7 Appendix

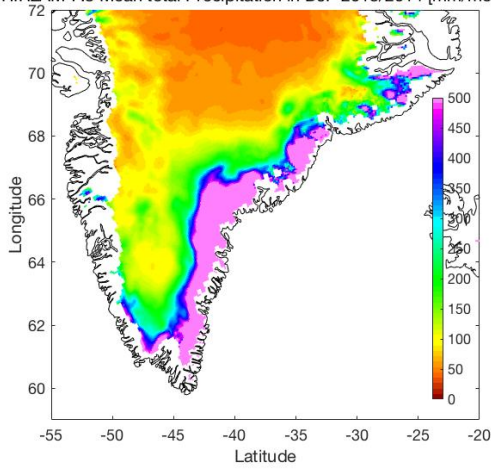
Seasonal average total precipitation in [mm/3-months] from HIRHAM5 and HIRLAM 7.3 along with the difference between them, the anomalies. December January February (DJF), Mars April May (MAM), June July August (JJA), and September October November (SON).

2014 HIRHAM5

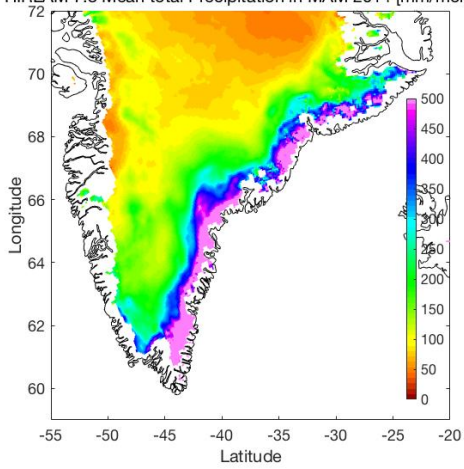


2014 HIRLAM 7.3

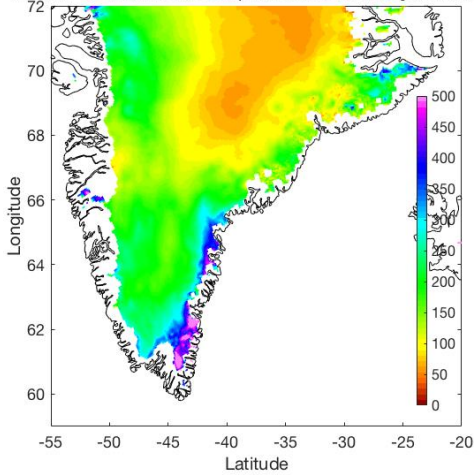
HIRLAM 7.3 Mean total Precipitation in DJF 2013/2014 [mm/months]



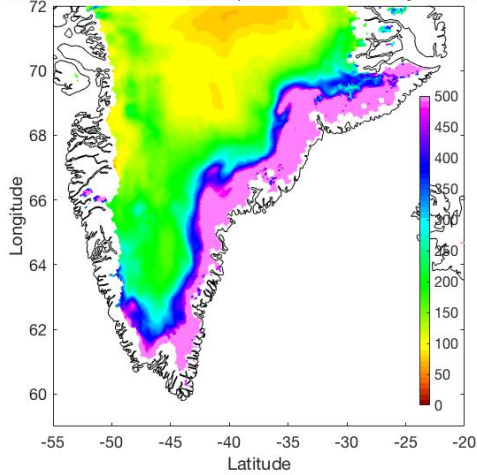
HIRLAM 7.3 Mean total Precipitation in MAM 2014 [mm/months]



HIRLAM 7.3 Mean total Precipitation in JJA 2014 [mm/months]

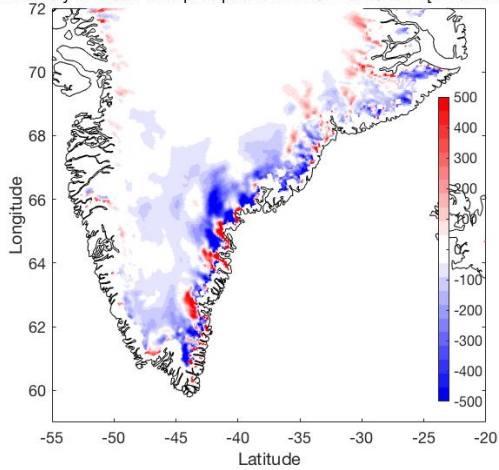


HIRLAM 7.3 Mean total Precipitation in SON 2014 [mm/months]

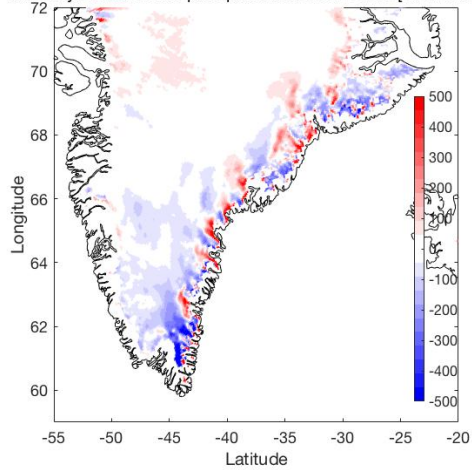


2014 Seasonal Anomalies

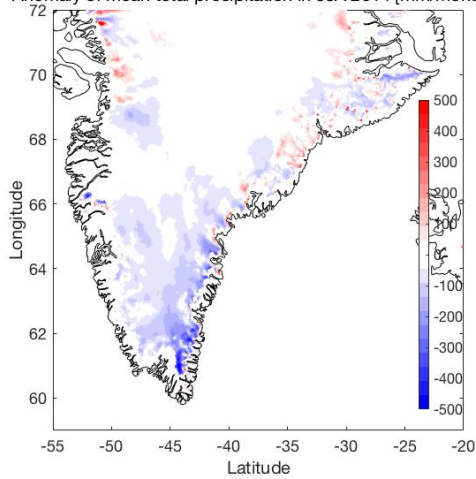
Anomaly of mean total precipitation in DJF 2013/2014 [mm/months]



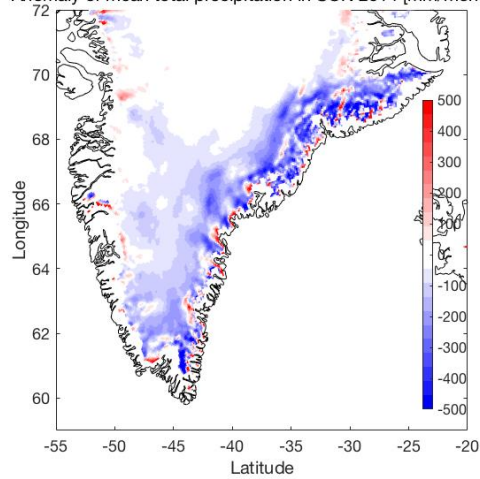
Anomaly of mean total precipitation in MAM 2014 [mm/months]



Anomaly of mean total precipitation in JJA 2014 [mm/months]

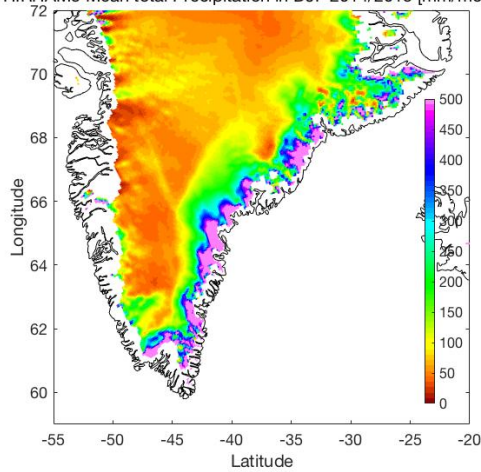


Anomaly of mean total precipitation in SON 2014 [mm/months]

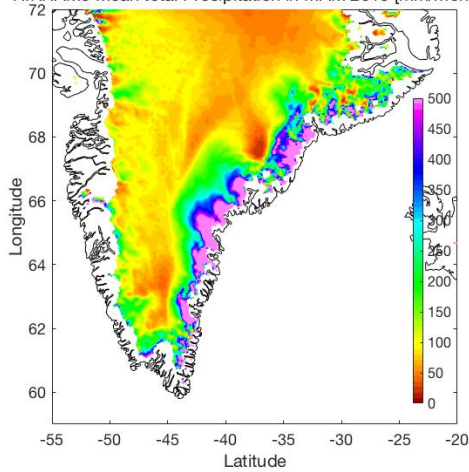


2015 HIRHAM5

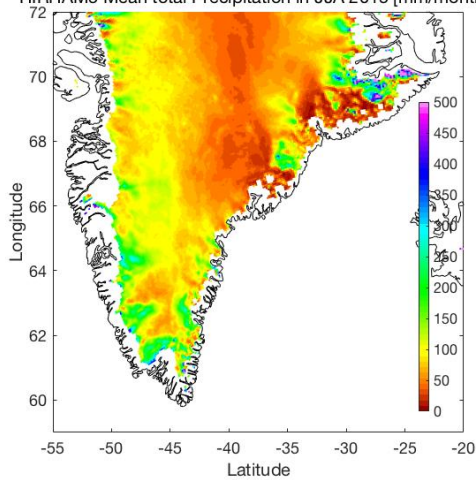
HIRHAM5 Mean total Precipitation in DJF 2014/2015 [mm/months]



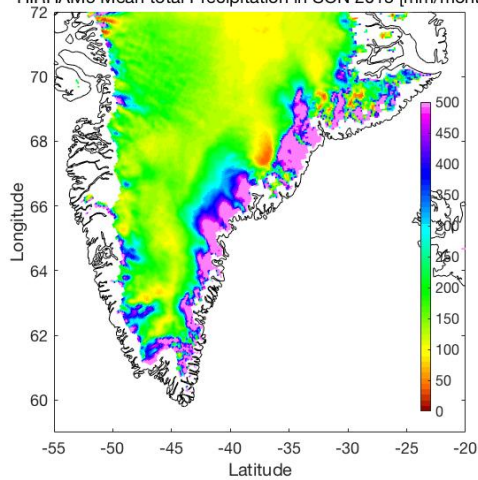
HIRHAM5 Mean total Precipitation in MAM 2015 [mm/months]



HIRHAM5 Mean total Precipitation in JJA 2015 [mm/months]

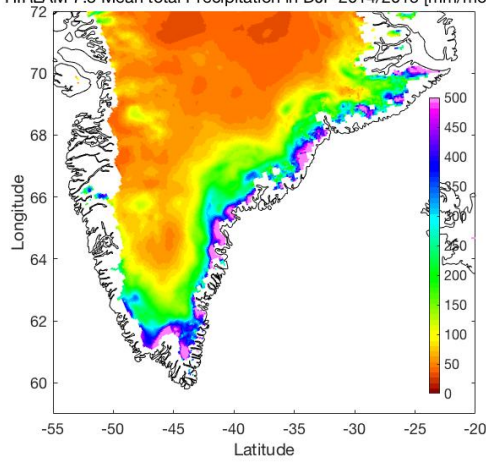


HIRHAM5 Mean total Precipitation in SON 2015 [mm/months]

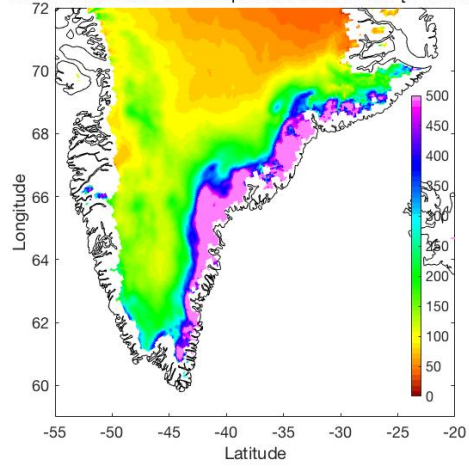


2015 HIRLAM 7.3

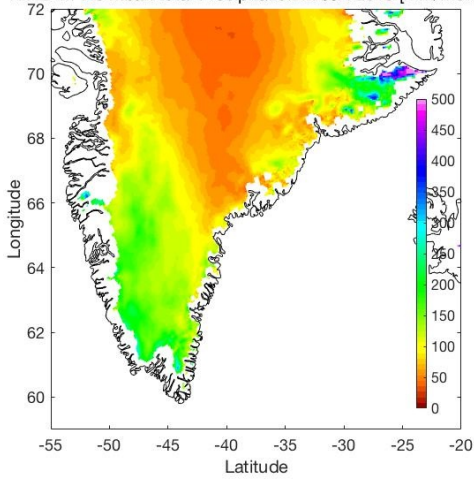
HIRLAM 7.3 Mean total Precipitation in DJF 2014/2015 [mm/months]



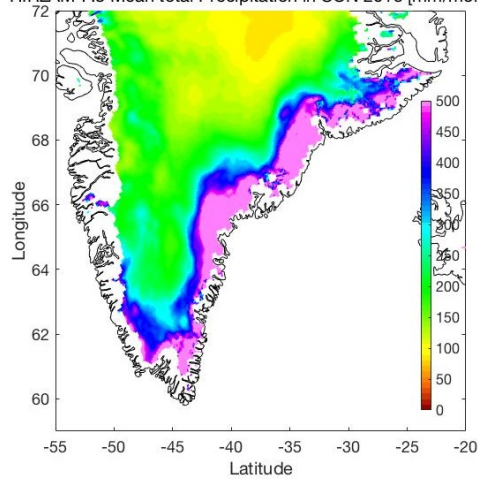
HIRLAM 7.3 Mean total Precipitation in MAM 2015 [mm/months]



HIRLAM 7.3 Mean total Precipitation in JJA 2015 [mm/months]

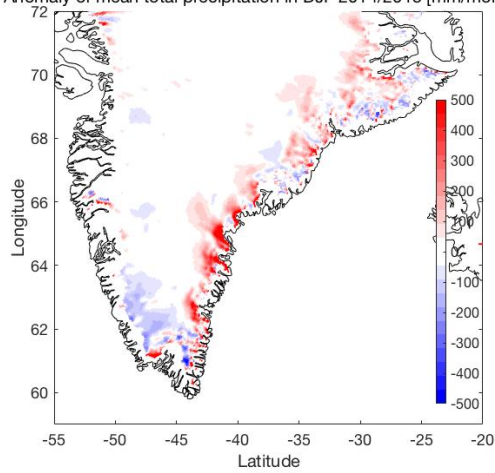


HIRLAM 7.3 Mean total Precipitation in SON 2015 [mm/months]

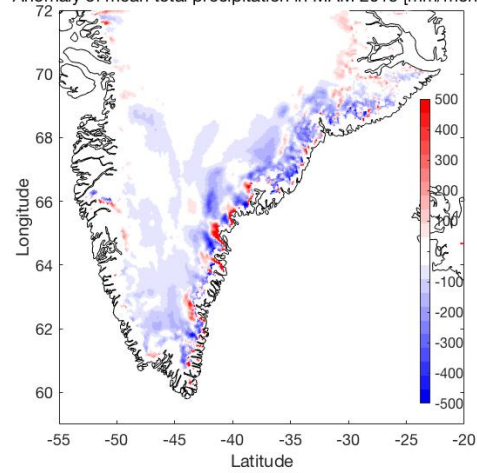


2015 Seasonal Anomalies

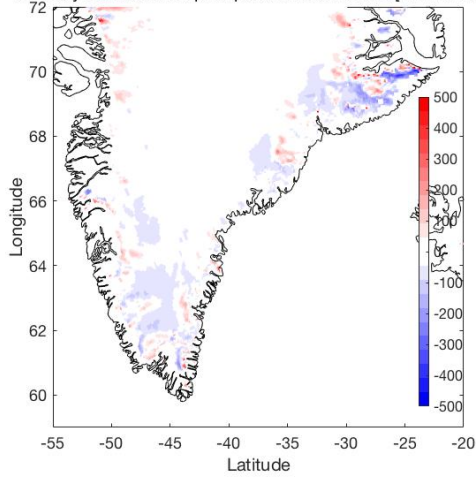
Anomaly of mean total precipitation in DJF 2014/2015 [mm/months]



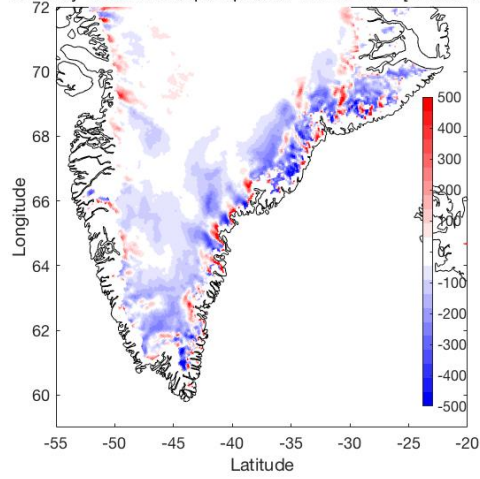
Anomaly of mean total precipitation in MAM 2015 [mm/months]



Anomaly of mean total precipitation in JJA 2015 [mm/months]

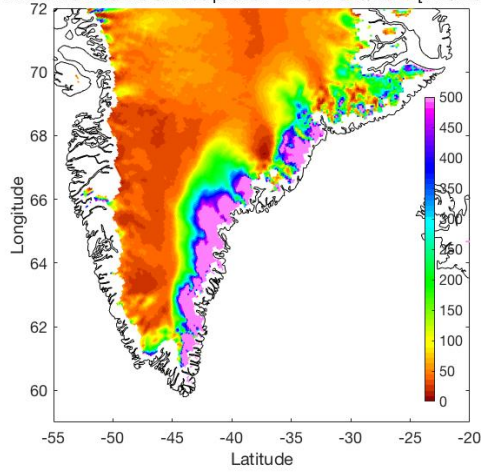


Anomaly of mean total precipitation in SON 2015 [mm/months]

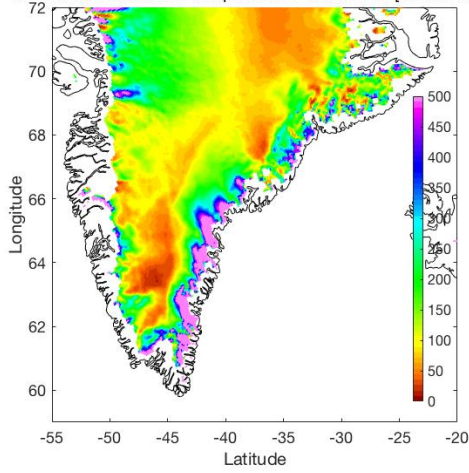


2016 HIRHAM5

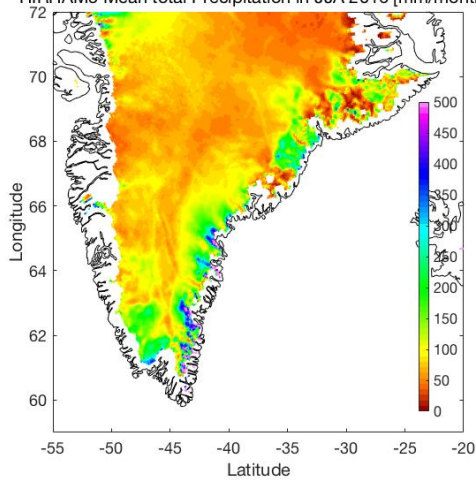
HIRHAM5 Mean total Precipitation in DJF 2015/2016 [mm/months]



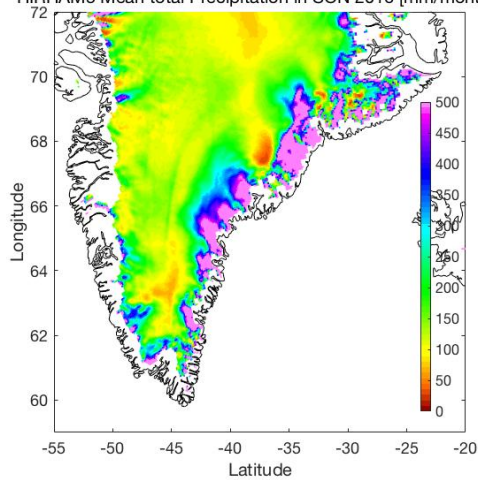
HIRHAM5 Mean total Precipitation in MAM 2016 [mm/months]



HIRHAM5 Mean total Precipitation in JJA 2016 [mm/months]

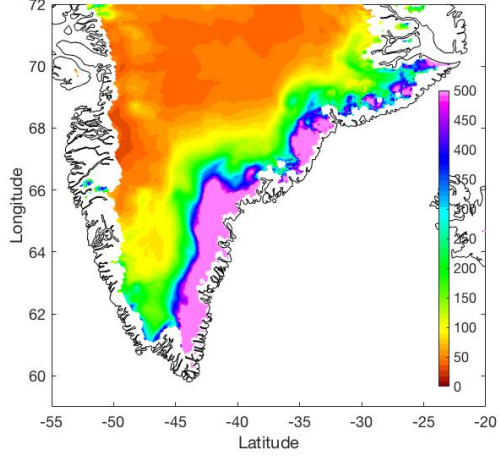


HIRHAM5 Mean total Precipitation in SON 2016 [mm/months]

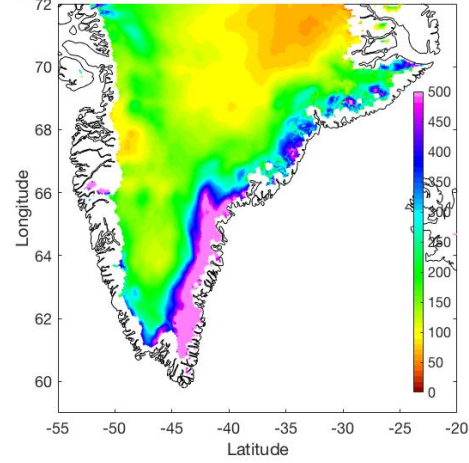


2016 HIRLAM 7.3

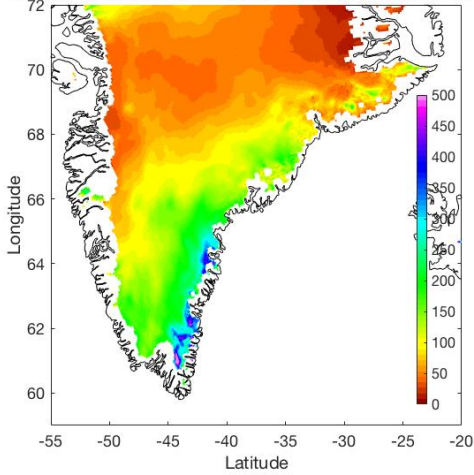
HIRLAM 7.3 Mean total Precipitation in DJF 2015/2016 [mm/months]



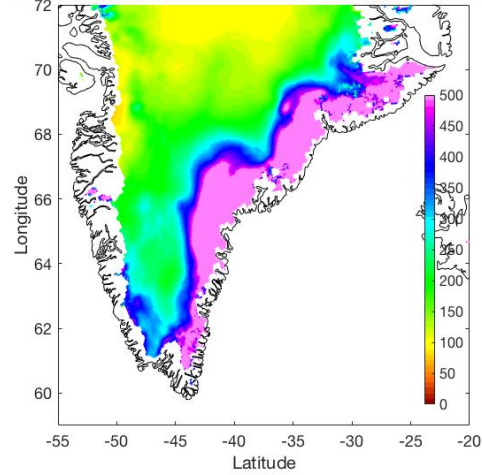
HIRLAM 7.3 Mean total Precipitation in MAM 2016 [mm/months]



HIRLAM 7.3 Mean total Precipitation in JJA 2016 [mm/months]

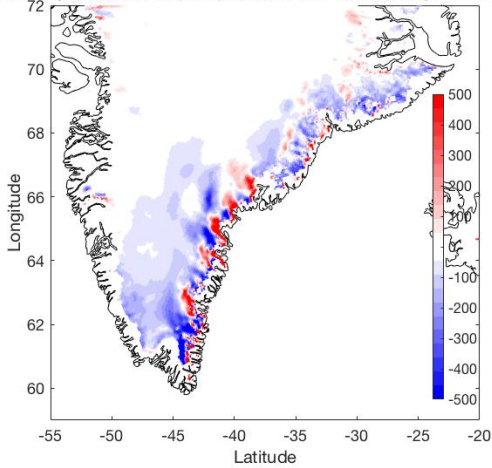


HIRLAM 7.3 Mean total Precipitation in SON 2016 [mm/months]

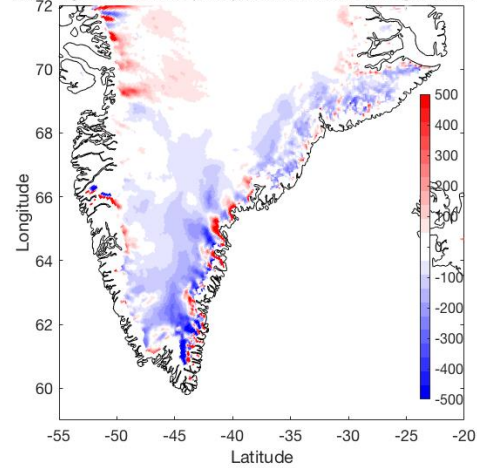


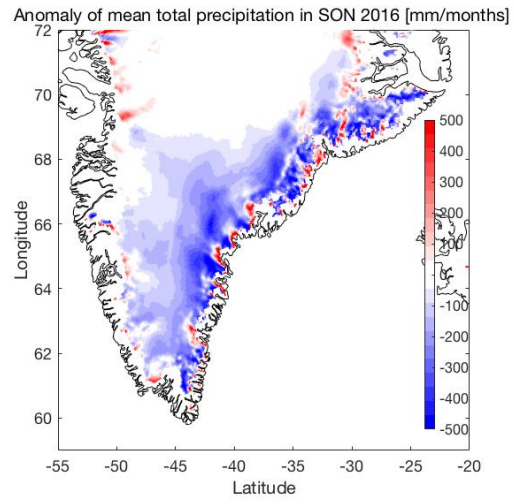
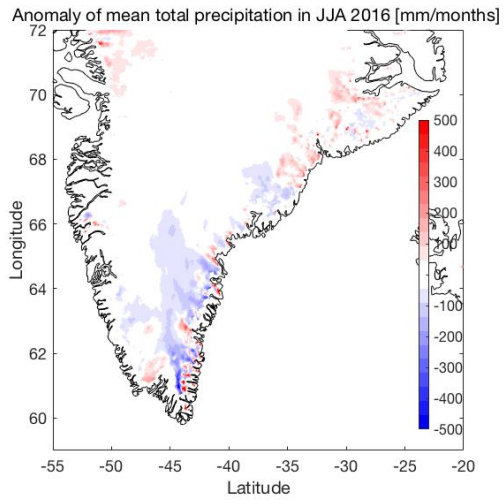
2016 Seasonal Anomalies

Anomaly of mean total precipitation in DJF 2015/2016 [mm/months]



Anomaly of mean total precipitation in MAM 2016 [mm/months]





Examples of MATLAB script used for the map plots. The first is for polaraxis map plots, and the second script is for the anomaly plots.

```

Clear all;

% load variables
file = '/Users/Rebecca/Desktop/MATLAB/DMI-HIRHAM5_2014-
_2016_PR_MM_remapbil_TS_glmask.nc';
ncid = netcdf.open(file,'NC_NOWRITE');
lon = double(ncread(file,'lon'));
lat = double(ncread(file,'lat'));
rainfall = double(ncread(file,'var232'));
netcdf.close(ncid);

%Get the land sea mask here (sea is a NAN)
fil = '/Users/Rebecca/Desktop/MATLAB/DMI-HIRHAM5_2014-
_2016_PR_MM_remapbil_TS_glmask.nc';
ncid = netcdf.open(fil, 'NC_NOWRITE' );

%glacier mask
gm = double(ncread(fil,'var232'));
gm(gm>=0.5) = 1; gm(gm<0.5) = NaN; %gm = gm';
netcdf.close(ncid);

% map init
hFig = figure(1); set(hFig, 'Position', [100 20 700 600])
clf; axes('position', [0.0 0.08 1.0 0.9]);
worldmap('landareas.shp',[min(lat(:)) max(lat(:))],[min(lon(:)) max(lon(:))],'line')
setm(gca,'Grid','on','GColor',[0.5 0.5
0.5],'GLineStyle',':','Frame','on','MeridianLabel','on','ParallelLabel','on','MLabelLocation',10,'P
LabelLocation',5,'MapProjection','eqdconicstd','FontSize',16);

% colormap def
cmap = [0 100 0; 52 160 52; 60 179 113; 120 195 120; 180 210 130; 240 230 140; 230 200
110; 215 165 80; 205 133 63; 210 105 30; 185 90 25; 139 69 19;]./255;

% map plot
surfacem(lat,lon,rainfall.*gm);
caxis ([0 300])
colormap(cmap);
title('HIRHAM5 Monthly mean precipitation over the period 2014-2016
[mm/month]','FontSize',18,'FontWeight','normal');

% Coastlines of the world!
load('/Users/Rebecca/Desktop/MATLAB/kystlinie_highres.mat');
plot3m(lat_kyst,lon_kyst,99999999,'k-','LineWidth',0.1);

% add colorbar
h = colorbar('horizontal','position',[0.20 0.84 0.60 0.03],'XTick',0:50:300);

```

```

%This is for the ANOMALY precipitation
clear all;

%use this file for lats and lons
fil = 'Users/Rebecca/Desktop/MATLAB/H5-
H_2016_PR_OCTOBER_TIMMEAN_gmask.nc';
ncid = netcdf.open(fil, 'NC_NOWRITE');
lon_grid = double(ncread(fil,'lon'));
lat_grid = double(ncread(fil,'lat'));
% here is the tricky part with adding lines for Greenland border
Lat = lat_grid ;
Lon = lon_grid ;
load('Users/Rebecca/Desktop/MATLAB/latlon_Greenland.mat');
LatG = lat; LonG = lon;

% define figure window size
hFig = figure(1);
set(hFig, 'Position', [100 100 600 584])
netcdf.close(ncid);

% get the variable you're interested in here
fil = 'Users/Rebecca/Desktop/MATLAB/H5-
H_2016_PR_OCTOBER_TIMMEAN_gmask.nc';
ncid = netcdf.open(fil, 'NC_NOWRITE');
PR_d = double(ncread(fil,'var232'));
PR = PR_d
netcdf.close(ncid);

% Get the land sea mask here (sea is a NAN)
fil = 'Users/Rebecca/Desktop/MATLAB/cl00010000.nc';
ncid = netcdf.open(fil, 'NC_NOWRITE');
lsm = double(ncread(fil,'var81'));
lsm(lsm<0.5) = NaN; lsm(lsm>=0.5) = 1;

%glacier mask
gm = double(ncread(fil,'var232'));
gm(gm>=0.5) = 1; gm(gm<0.5) = NaN; %gm = gm';
netcdf.close(ncid);

% Coastlines of the world!
load('Users/Rebecca/Desktop/MATLAB/kystlinie_highres.mat');

clf; axes('position', [0.04 0.10 0.92 0.82]);
clf; surface(lon_grid,lat_grid,PR,'EdgeColor','none')

% set upper lower limits of plot values with caxis
caxis ([-10 10]); %PR

cmap = colormap(b2r(0,10));
hold on;
% plot border
load 'Users/Rebecca/Desktop/MATLAB/latglong.mat'
plot(LatG,LonG,'k-','LineWidth',1)
hold on;
plot3(lon_kyst,lat_kyst,500*ones(size(lon_kyst)),'-k')

%sets the lon + lat limits to make the plot look nice
latlim = [-55 -20];
lonlim = [59 72];
axis tight; xlim(latlim); ylim(lonlim); box on
|
% puts in and positions a vertical legend, change these numbers for
% horizontal one 'horiz'
colorbar('vertical','position',[0.82 0.15 0.02 0.60],'YTick',-10:2:10);
text(7,60,'Mean Precipitation [mm/day]','FontSize',18,'FontWeight','normal','Rotation',90)
title('Anomaly of daily mean precipitation in October 2016 [mm/day]
','FontSize',18,'FontWeight','normal')
xlabel('Latitude', 'FontSize',8,'FontWeight','normal')
ylabel('Longitude', 'FontSize',8,'FontWeight','normal')
set(gca,'FontSize',18); set(gcf,'PaperPositionMode','auto');

```

C Shell Scripting example, of extracting information and converting units of a NetCDF file to an array in a textfile. Used for the plotted diagrams in the report.

```
#
# Calculates monthly time series of the variables
#
#####
set workdir = '/local_data/climate01/student1/hirham/OUT'
set datadir = '/local_data/climate01/student1/hirham/OUT/NETCDF/monthlymeans'

set years = 2014
set yearf = 2016
set startname = ERAI

cd $datadir

foreach per (MM)

foreach var (PR RAIN SNFALL)
  gunzip ${ ERAI }_${years}_${yearf}_${var}_${per}.nc.gz

  #Multiply with conversion factor, to change kg m-2 day-1 to GT year-1
  #including conversion when multiplying with area in km2
  #kg/m2/day*km2*365days/year*10e6m2/km2*10e-12GT/kg
  cdo mulc,0.000365 ${ERAI}_${years}_${yearf}_${var}_${per}.nc
  S${var}_${per}_conv.nc

  #Multiply with the glacier:
  cdo mul glmask_GR6b.nc S${var}_${per}_conv.nc S${var}_${per}_conv_mask.nc

  #Multiply with the area grid (in km2)
  cdo mul area.nc S${var}_${per}_conv_mask.nc S${var}_${per}_conv_mask_area.nc

  # Do the sum over all grid points (there are values only over the glacier and the rest are 0)
  cdo fldsum S${var}_${per}_conv_mask_area.nc S${var}_${per}_conv_mask_area total.nc

  #put the time series into an ascii file
  cdo info S${var}_${per}_conv_mask_area_total.nc | grep -v Mean | awk '{print $10}' >
  timeseries_${var}_${per}.txt

end

end
```